Disturbance Observer Design Based on Linearized Vehicle Model

for Unequal Tractive/Braking Force Identification

Jiwon Oh[1*], Seibum Choi[2] and Daeil Kim[3]

[1] Department of Mechanical Engineering, KAIST, Daejeon, 305-701, Korea
(Tel : +82-42-350-4160; E-mail: jwo@kaist.ac.kr) * Corresponding author
[2] Department of Mechanical Engineering, KAIST, Daejeon, 305-701, Korea
(Tel : +82-42-350-4120; E-mail: sbchoi@kaist.ac.kr)
[3] Department of Mechanical Engineering, KAIST, Daejeon, 305-701, Korea
(Tel : +82-42-350-4160; E-mail: kemadd@kaist.ac.kr)

Abstract: The study focuses on the methodology to take the effect of the unequal longitudinal tire forces into consideration to reinforce the accuracy of the linearized vehicle model, also known as the bicycle model. Using the estimated front and rear cornering stiffness values obtained through an adaptive scheme, the conventional bicycle model is analyzed. By forming the inverse bicycle model, a disturbance observer to estimate the unconsidered amount of yaw acceleration caused by the discrepancy between the left and right longitudinal tire forces is designed. The accuracy of the modified bicycle model is verified using CarSim, a well-known vehicle dynamics testing software, via comparing the estimated states of the conventional and modified vehicle model.

Keywords: vehicle dynamics, disturbance observer, adaptive scheme, estimation, stability

1. INTRODUCTION

With the rapid growth of the computerized technology, the vehicle safety control system such as braking control, stability control, and lateral control algorithms [1, 2] is considered inseparable from the production vehicles. The real-time application of these algorithms can significantly increase the level of safety by assisting the drivers to obtain the desirable vehicle motion.

However, the reliable performance of the mentioned algorithms only comes with reliable vehicle states on which the control systems rely. For example, the ESP (electronic stability program) often requires the accurate side slip angle information in order to produce the appropriate amount of yaw moment for obtaining the desired vehicle attitude. Here, the side slip angle, closely related to the lateral vehicle velocity, is not easily attainable without an expensive set of sensors. Thus, vehicle state observers are used to estimate the required vehicle states.

For this purpose, the related previous works [3, 4] used the linearized vehicle model, also known as bicycle model. Sometimes, this model-based observer was used along with the direct integral of the sensor kinematics [1, 4, 5]. Even in such cases, however, the use of the vehicle model is inevitable, since the drift issue related with the direct integration must be compensated.

Thus, if the accuracy of the vehicle model can be improved, improvement in the state estimation accuracy and the control system performance that follow can be expected as well. For this purpose, the paper focuses on including the vehicle dynamics component which had not been considered in the conventional bicycle model: discrepancy between the left and right longitudinal tire forces.

Previous efforts to modify the conventional bicycle model attempted to consider the roll dynamics [6, 7].

With the addition of the suggested modification on top of the existing modified models, significant increase in

Nomenclature

m : vehicle mass
g : gravitational constant
h : C.G. height
l_f : distance between C.G. and front axle
l_r : distance between C.G. and rear axle
L : distance between front and rear axle
I_z : moment of inertia about z-axis
α_f : front tire slip angle
α_r : rear tire slip angle
C_f : front tire cornering stiffness
C_r : rear tire cornering stiffness
δ_f : front tire steering angle
β : side slip angle at C.G
v_x : longitudinal velocity at C.G.
v_y : lateral velocity at C.G.
v_z : vertical velocity at C.G.
a_y : lateral acceleration at C.G.
r : yaw rate measured at C.G.
F_{yf} : front axle lateral tire force
F_{yr} : rear axle lateral tire force
F_{zf} : front axle vertical tire force
F_{zr} : rear axle vertical tire force

the model accuracy on the split road friction condition is anticipated. In addition, with the unconsidered yaw moment estimation available, the information can be useful for the split-mu detection and torque steer compensation. In order to verify the positive effect of the modification, simulations on the split-mu road surface are done, and the estimation of the yaw moment

caused purely by the unbalanced longitudinal tire forces is presented using CarSim.

The remaining parts of the paper are organized as follows. Section 2 deals with how the vehicle model is modified compared to the conventional bicycle model. This section includes the explanations on disturbance observer for estimating the unconsidered yaw moment, and cornering stiffness adaptation. Section 3 presents the stability analysis of the observer with the disturbance rejection applied. Section 4 displays the simulation results that show the vehicle state and disturbance estimation performance.

2. MODIFIED VEHICLE MODEL DESIGN
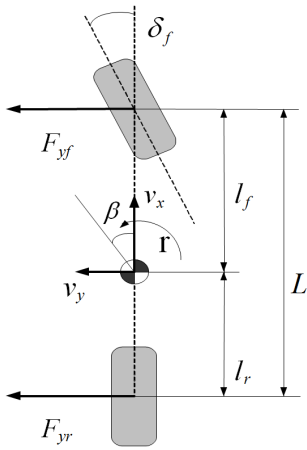
2.1 Conventional Bicycle Model

Fig. 1 Bicycle model.

The above figure is the bicycle model representation of the vehicle which describes the lateral dynamics of a vehicle. Its popularity comes from the considerable amount of reduction in the required computational efforts for the state identification compared to those required in the full vehicle model.

In general, the representation of the bicycle model is given as follows.

$$\dot{x} = Ax + Bu \tag{1}$$

where $x = \begin{bmatrix} \beta \\ r \end{bmatrix}$, $u = \delta_f$,

$$A = \begin{bmatrix} a_{11} & a_{12} \\ a_{21} & a_{22} \end{bmatrix}$$

$$= \begin{bmatrix} -\dfrac{(C_f + C_r)}{mv_x} & -\dfrac{(C_f l_f - C_r l_r)}{mv_x^2} - 1 \\ -\dfrac{(C_f l_f - C_r l_r)}{I_z} & -\dfrac{(C_f l_f^2 + C_r l_r^2)}{I_z v_x} \end{bmatrix},$$

and $B = \begin{bmatrix} b_1 \\ b_2 \end{bmatrix} = \begin{bmatrix} \dfrac{C_f}{mv_x} \\ \dfrac{C_f l_f}{I_z} \end{bmatrix}$

As its name suggests, the bicycle model deals with the dynamics under the assumption that the left and right side of the vehicle experience the same behavior.

Such assumption, however, does not always hold. Some of the most critical limitations of using the bicycle model relate to the cases in which roll dynamics and unbalanced longitudinal tire forces are involved. Regarding the latter case, no attempt is made to modify the bicycle model to consider the yaw moment generated purely caused by the difference between the left and the right longitudinal tire forces. This is illustrated in fig. 2, where the yaw moment generated due to the difference between F_{yf} and F_{yr} is accounted in the conventional bicycle model, whereas that between F_{xL} and F_{xR} is not.

Fig. 2 Two major causes of yaw acceleration.

2.2 Disturbance Observer Approach

As discussed in the previous section, model inaccuracy on the split-mu surface is a major shortcoming when using the conventional vehicle model. Therefore, the suggested work attempts to improve on this issue, and the main contribution of this paper is the unbalanced longitudinal tire force estimation using disturbance observer.

Exploiting the fact that the conventional vehicle model does not fully take both causes of yaw moment into account, designing the disturbance observer gives an advantage on estimating the unconsidered component of the cause of yaw moment.

As fig. 3 shows, the plant, or the vehicle, is modeled with the conventional vehicle model. Then the inverse dynamics of the bicycle model is used to form the estimation of the input, which is compared with the

compensated input to the plant – tire steering angle. This difference is fed back to be subtracted from the actual input variable, which forms the compensated steering angle.
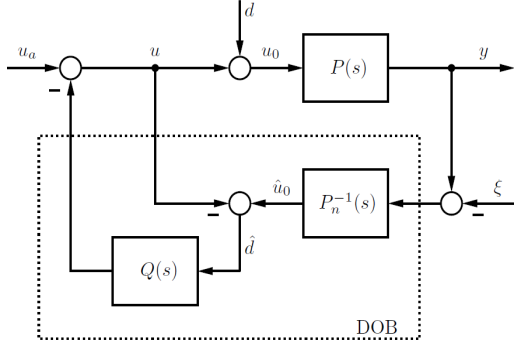

Fig. 3 Block diagram of the disturbance observer.

Considering the yaw moment caused by the unbalanced longitudinal tire forces as the disturbance, the disturbance term is added to (1) as the following.

$$\dot{x} = Ax + Bu + M \tag{2}$$

where $M = \begin{bmatrix} 0 \\ d \end{bmatrix}$

Here, the physical meaning of d indicates the yaw acceleration. Thus it is included only in the yaw acceleration dynamics, under the assumption that the unbalanced longitudinal force only induces yaw moment and has no influence on the vehicle side slip angle. Now let

$$d = \frac{C_f l_f}{I_z} d^* \tag{3}$$

Eq. (3) enables the disturbance term to merge with the input variable. Physically this makes sense, since the yaw moment in fact gives the steering effect.

$$\begin{bmatrix} \dot{\hat{\beta}} \\ \dot{\hat{r}} \end{bmatrix} = \begin{bmatrix} \dfrac{-(C_f + C_r)}{mv_x} & \dfrac{-(C_f l_f - C_r l_r)}{mv_x^2} - 1 \\ \dfrac{-(C_f l_f - C_r l_r)}{I_z} & -\dfrac{(C_f l_f^2 + C_r l_r^2)}{I_z v_x} \end{bmatrix} \begin{bmatrix} \hat{\beta} \\ \hat{r} \end{bmatrix}$$
$$+ \begin{bmatrix} \dfrac{C_f}{mv_x} \delta_f \\ \dfrac{C_f l_f}{I_z}(\delta_f + \hat{d}^*) \end{bmatrix} + K \begin{bmatrix} r - \hat{r} \\ a_y - \hat{a}_y \end{bmatrix} \tag{4}$$

Eq. (4) shows the state estimator using the disturbance observer. K is the observer feedback gain matrix [8]. The observer feedback term is obtained as the following.

$$y = \begin{bmatrix} r \\ a_y \end{bmatrix}, \ \hat{y} = \begin{bmatrix} \hat{r} \\ \hat{a}_y \end{bmatrix} = C \begin{bmatrix} \hat{\beta} \\ \hat{r} \end{bmatrix} + D,$$

where $C = \begin{bmatrix} 0 & 1 \\ a_{11}v_x & (a_{12}+1)v_x \end{bmatrix}$ and $D = \begin{bmatrix} 0 \\ b_1 v_x \end{bmatrix}$. $\tag{5}$

Now, the disturbance $\hat{d}^*$ is obtained as the following.

$$I_z \dot{r} - (C_r l_r - C_f l_f)\hat{\beta} + \frac{C_f l_f^2 + C_r l_r^2}{v_x} r = l_f C_f \hat{\delta}_f \tag{6}$$

Since the inverse dynamics must be formed, estimation of the input $-\hat{\delta}_f-$ is calculated according to the relationship shown in eq. (6). The estimation of the disturbance is found as follows.

$$\hat{d}^* = \hat{\delta}_f - \delta_f$$

$$= \frac{I_z \dot{r} - (C_r l_r - C_f l_f)\hat{\beta} + \dfrac{C_f l_f^2 + C_r l_r^2}{v_x} r}{l_f C_f} - \delta_f \tag{7}$$

To assure that the system is causal, $\hat{d}^*$ finally obtained as shown next.

$$\dot{\hat{d}}^* = -\eta \left(\hat{d}^* - \frac{I_z \dot{r} - (C_r l_r - C_f l_f)\hat{\beta} + \dfrac{C_f l_f^2 + C_r l_r^2}{v_x} r}{l_f C_f} + \delta_f \right)$$

where η is the gain. $\tag{8}$

2.3 Cornering Stiffness Adaptation

Cornering stiffness adaptation is crucial for the observer system, both because it raises the lateral dynamics modeling accuracy in the bicycle model, and because it works as the multiplier for the unconsidered yaw moment estimation as expressed in eq. (3).

Design of the adaptive scheme begins from the following relationship.

$$\beta = -\frac{F_{yf}}{C_f} + \delta_f - \frac{l_f}{v_x} r = -\frac{F_{yr}}{C_r} + \frac{l_r}{v_x} r \tag{9}$$

Rearranging the above equation and substituting the cornering stiffness values by the sum of the nominal and unknown values normalized by the vertical tire load, the following is reached.

$$\frac{F_{yf}}{F_{zf}}\left(\left(\frac{1}{\overline{C}_f}\right)_n + \zeta_f\right) - \frac{F_{yr}}{F_{zr}}\left(\left(\frac{1}{\overline{C}_r}\right)_n + \zeta_r\right) = \delta_f - \frac{l_f + l_r}{v_x} r \tag{10}$$

Now separating the unknowns and the knowns leads to the following.

$$\zeta \equiv \frac{F_{yf}}{F_{zf}} \zeta_f - \frac{F_{yr}}{F_{zr}} \zeta_r$$

$$= \delta_f - \frac{l_f + l_r}{v_x} r - \frac{F_{yf}}{F_{zf}}\left(\frac{1}{\overline{C}_f}\right)_n + \frac{F_{yr}}{F_{zr}}\left(\frac{1}{\overline{C}_r}\right)_n \tag{11}$$

The steer angle, longitudinal velocity, and yaw rates are assumed given, and the lateral tire forces are calculated based on the bicycle model using the yaw rate and lateral acceleration sensors. The normalizing variables – vertical loads – are obtained using a 6D IMU, but if it is

not available, the adaptive scheme can be formed without normalization process as well. After low pass filtering with the filter gain η to make the error dynamics causal, the following is reached.

$$\dot{\zeta} = -\eta \left(\hat{\zeta} - \frac{F_{yf}}{F_{zf}} \hat{\zeta}_f + \frac{F_{yr}}{F_{zr}} \hat{\zeta}_r \right) \qquad (12)$$

Now the adaptive laws that identify the unknown parts of the front and rear cornering stiffness values are designed as the following.

$$\dot{\zeta}_f = \eta \eta_f \frac{F_{yf}}{F_{zf}} \varepsilon_n \qquad (13)$$

$$\dot{\zeta}_r = -\eta \eta_r \frac{F_{yr}}{F_{zr}} \varepsilon_n \qquad (14)$$

where η_f and η_r are adaptation gains and $\varepsilon_n \triangleq \zeta - \hat{\zeta}$. Refer to [9] for further details on the background principles and the stability analysis of the adaptation.

3. STABILITY ANALYSIS

Inclusion of the disturbance estimation dynamics to eq. (2) gives the following expanded model, under the assumption that the disturbance varies slowly.

$$\dot{x} = Ax + B\delta_f \qquad (15)$$

where now $x = \begin{bmatrix} \beta \\ r \\ d^* \end{bmatrix}$, $B = \begin{bmatrix} \dfrac{C_f}{mv_x} \\ \dfrac{C_f l_f}{I_z} \\ 0 \end{bmatrix}$, and

$$A = \begin{bmatrix} -\dfrac{(C_f + C_r)}{mv_x} & \dfrac{-(C_f l_f - C_r l_r)}{mv_x^2} - 1 & 0 \\ \dfrac{-(C_f l_f - C_r l_r)}{I_z} & -\dfrac{(C_f l_f^2 + C_r l_r^2)}{I_z v_x} & \dfrac{C_f l_f}{I_z} \\ 0 & 0 & 0 \end{bmatrix}.$$

Recall the disturbance estimation law dealt in eq. (8). Its inclusion in eq. (4) gives the observer dynamics as shown next.

$$\dot{\hat{x}} = A'\hat{x} + B'\delta_f + K(y - \hat{y}) + R \qquad (16)$$

where $\hat{x} = \begin{bmatrix} \hat{\beta} \\ \hat{r} \\ \hat{d}^* \end{bmatrix}$, $B' = \begin{bmatrix} \dfrac{C_f}{mv_x} \\ \dfrac{C_f l_f}{I_z} \\ -\eta \end{bmatrix}$, R= $\begin{bmatrix} 0 \\ 0 \\ \eta \dfrac{I_z \dot{r} + \dfrac{C_f l_f^2 + C_r l_r^2}{v_x} r}{l_f C_f} \end{bmatrix}$

and

$$A' = \begin{bmatrix} -\dfrac{(C_f + C_r)}{mv_x} & \dfrac{-(C_f l_f - C_r l_r)}{mv_x^2} - 1 & 0 \\ \dfrac{-(C_f l_f - C_r l_r)}{I_z} & -\dfrac{(C_f l_f^2 + C_r l_r^2)}{I_z v_x} & \dfrac{C_f l_f}{I_z} \\ \dfrac{-\eta(C_r l_r - C_f l_f)}{l_f C_f} & 0 & -\eta \end{bmatrix}.$$

For the sake of stability analysis with taking the disturbance variable into account as well, the output matrix and the feedback gain matrix are expanded so that C is a 2×3 matrix with the third column zero and K is a 3×2 matrix with the third row zero. Then eq. (16) can be expressed as follows.

$$\dot{\hat{x}} = A'\hat{x} + B'\delta_f + K(C\tilde{x} + D) + R \qquad (17)$$

where $\tilde{x} = x - \hat{x}$.

Now, if eq. (8) is expanded using the yaw acceleration dynamics shown in eq. (15), then the following is reached.

$$\dot{\hat{d}}^* = \eta \frac{I_z}{l_f C_f} \left(\frac{-(C_f l_f - C_r l_r)}{I_z} \beta - \frac{(C_f l_f^2 + C_r l_r^2)}{I_z v_x} r \right. \\ \left. + \frac{C_f l_f}{I_z} d^* + \frac{C_f l_f}{I_z} \delta_f \right)$$
$$- \eta \hat{d}^* - \eta \frac{(C_r l_r - C_f l_f)}{l_f C_f} \hat{\beta} + \eta \frac{C_f l_f^2 + C_r l_r^2}{l_f C_f v_x} r - \eta \delta_f$$
$$= \eta \tilde{d}^* + \eta \frac{-(C_f l_f - C_r l_r)}{l_f C_f} \tilde{\beta}$$

then $$\dot{\tilde{d}}^* = -\eta \tilde{d}^* + \eta \frac{(C_f l_f - C_r l_r)}{l_f C_f} \tilde{\beta} \qquad (18)$$

Using eq. (18), subtracting eq. (17) from (15) gives the following error dynamics.

$$\dot{\tilde{x}} = A'\tilde{x} - K(C\tilde{x} + D) \qquad (19)$$

$$K = \begin{bmatrix} a_{12} & 0 \\ \dfrac{-a_{21}(a_{12}+1)}{a_{11}} & \dfrac{a_{21}}{a_{11}v_x} \\ 0 & 0 \end{bmatrix} \qquad (20)$$

Choosing the observer feedback matrix K as shown in eq. (20) makes the state matrix $A' - KC$ Hurwitz.

4. SIMULATION RESULTS

Simulation for observer verification is done under three types of split-mu conditions: high split mu condition (left: 0.7, right: 1), high-medium split mu condition (left: 0.4, right: 1), and high low split mu condition (left: 0.1, right: 1). During the simulation,

accelerator and brake pedals are pressed to induce the unbalanced longitudinal forces. Open differential is used so that the torques transmitted to the left and right side of the differential are always the same (but longitudinal forces are different, because of the wheel inertia difference).
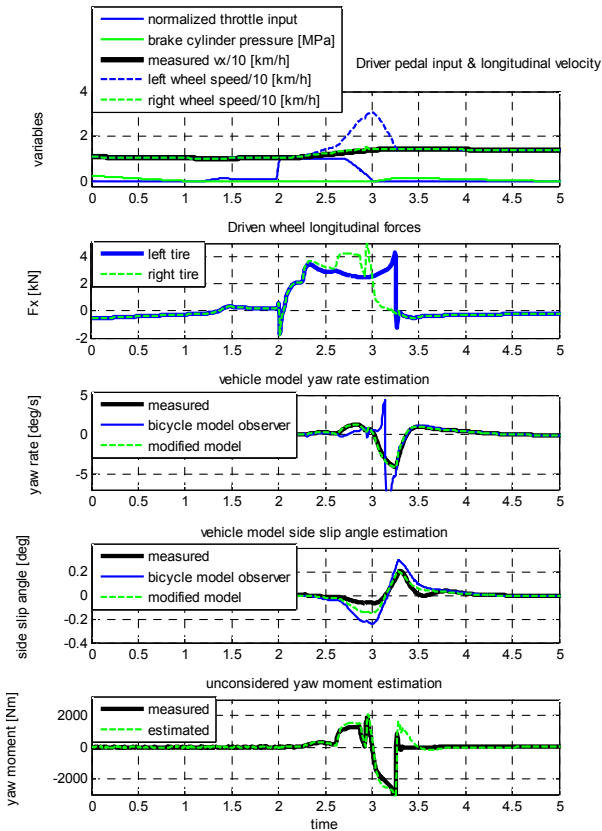

Fig. 4 Simulation result on 0.7-1 split mu condition.

As it can be seen in fig. 4 to 6, the modified bicycle model-based observer identifies the vehicle states with higher accuracy than the existing bicycle model-based observer [], and also simultaneously estimates the amount of yaw moment induced purely by the unbalanced longitudinal forces. The estimated yaw moment is plotted by multiplying the yaw moment of inertia to the estimated yaw acceleration value, d. Meanwhile, the measured yaw moment is plotted by multiplying half the wheel track to the difference in the longitudinal tire forces given by CarSim.

Although the conventional bicycle model-based observer uses the sensor measurement information (lateral acceleration and yaw rate) as its feedback, the estimation accuracy of the vehicle states decreased due to high amount of unconsidered component of yaw acceleration. The suggested algorithm effectively manages it as the disturbance which should be compensated. Even in the extreme case of wheel locking (the simulation was intentionally designed without ABS) as shown in fig. 6 between 8~10 second, the observer accurately estimates how much unbalanced longitudinal force the vehicle tires are generating.
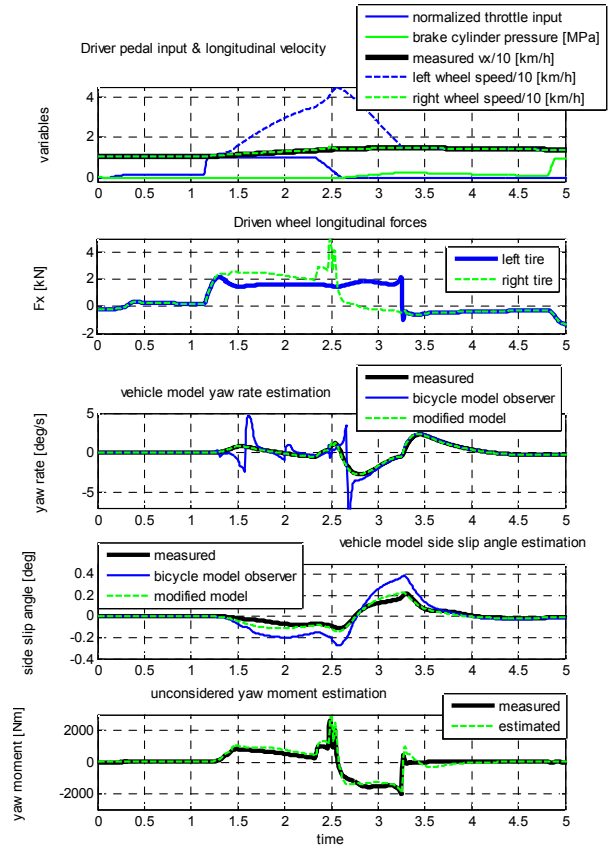

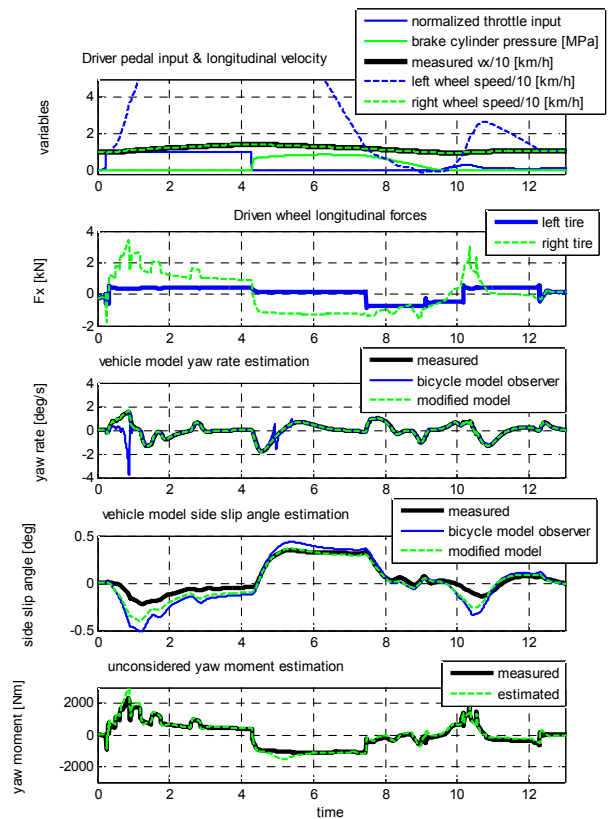Fig. 5 Simulation result on 0.4-1 split mu condition.

Fig. 6 Simulation result on 0.1-1 split mu condition.

5. Conclusion

The main objective of the suggested work is to improve the vehicle model-based estimation accuracy of the vehicle states. The major contributions of this paper which distinguish it from other previous works are the following. First, the work takes the effect of unbalanced longitudinal tire forces into account, so that the estimation accuracy of the yaw rate and side slip angle using the bicycle model observer is improved while maintaining the simplicity of the linear model. Secondly, the suggested algorithm is capable of estimating how much longitudinal tire forces are unbalanced and what the resulting yaw moment is. This may be practically helpful for detecting the split-mu condition for the safety control system applications.

REFERENCES

[1] Akitaka Nishio, et. al., "Development of Vehicle Stability Control System Based on Vehicle Sideslip Angle Estimation," *SAE Paper* No. 2001-01-0137.

[2] Scott Kimbrough., "Coordinated Braking and Steering Control for Emergency Stops and Accelerations," *Proceedings of the WAM ASME*, Atlanta, GA, pp. 229-244, 1991.

[3] Jim Farrelly and Peter Wellstead, "Estimation of Vehicle Lateral Velocity", *IEEE Conference on Control Applications . Proceedings*, p.552-557, 1996.

[4] Yoshiki Fukada, "Slip-Angle Estimation for Vehicle Stability Control", *Vehicle System Dynamics*, v.32, no.4, p.375-388, 1999.

[5] Hyeongcheol Lee, "Reliability Indexed Sensor Fusion and Its Application to Vehicle Velocity Estimation," *Transactions of the ASME*, Vol. 128, pp.236~243, 2006.

[6] Jihan Ryu, Eric J. Rossetter, and J. Christian Gerdes, "Vehicle Sideslip and Roll Parameter Estimation Using GPS", *Proceedings of AVEC 2002 6th International Symposium of Advanced Vehicle Control*, 2002.

[7] J. Oh and S.B. Choi, "Design of a New Multiple observer for Vehicle Velocity and Attitude Estimation," in the *Proceedings of the IASTED International Conference, control and Applications*, Vancouver, BC, Canada, pp. 102-109, 2011.

[8] H.W. Son, "A Study on Design of a Robust Vehicle Side-Slip Angle Observer using an Integration of Kinematic and Bicycle Model," *KSAE 2008 Annual Conference*, Daejeon, Korea, 2008.

[9] S.H. You, J.O. Hahn, H.C. Lee, "New Adaptive Approaches to Real-time Estimation of Vehicle Sideslip Angle," *Control Engineering Practice*, vol. 17, no. 12, 1367–1379, 2009.